Vertebral giant cell tumour of bone in a domestic shorthair cat

Authors: Caldero Carrete, Jordina, Tabanez, Joana, Civello, Alexander, and Rusbridge, Clare

Vertebral giant cell tumour of bone in a domestic shorthair cat

Jordina Caldero Carrete[1], Joana Tabanez[1], Alexander Civello[2] and Clare Rusbridge[1,3,4]

Abstract

Case summary A 10-year-old male neutered domestic shorthair cat was presented with a 5-month history of progressive non-ambulatory paraparesis. Initial vertebral column radiographs revealed an L2–L3 expansile osteolytic lesion. Spinal MRI showed a well-demarcated, compressive expansile extradural mass lesion affecting the caudal lamina, caudal articular processes and right pedicle of the second lumbar vertebra. The mass was hypointense/isointense on T2-weighted images, isointense on T1-weighted images and had mild homogeneous contrast enhancement after gadolinium administration. MRI of the remaining neuroaxis and CT of the neck, thorax and abdomen with ioversol contrast revealed no additional neoplastic foci. The lesion was removed by en bloc resection via a dorsal L2–L3 laminectomy, including the articular process joints and pedicles. Vertebral stabilisation was performed with titanium screws placed within L1, L2, L3 and L4 pedicles with polymethylmethacrylate cement embedding. Histopathology revealed an osteoproductive neoplasm composed of spindle and multinucleated giant cells without detectable cellular atypia or mitotic activity. On immunohistochemical evaluation, osterix, ionised calcium-binding adaptor molecule 1 and vimentin labelling were observed. Based on the clinical and histological features, a giant cell tumour of bone was considered most likely. Follow-up at 3 and 24 weeks postoperatively demonstrated significant neurological improvement. Postoperative full-body CT at 6 months showed instability of the stabilisation construct but absence of local recurrence or metastasis.

Relevance and novel information This is the first reported case of a giant cell tumour of bone in the vertebra of a cat. We present the imaging findings, surgical treatment, histopathology, immunohistochemistry and outcome of this rare neoplasm.

Keywords: Giant cell tumour of bone; neurology; surgical management; histopathology; immunohistochemistry; giant cell-rich osteosarcoma

Case description

A 10-year-old male neutered domestic shorthair cat was presented with a 5-month history of ambulatory paraparesis that progressed to non-ambulatory paraparesis 2 weeks prior to referral. Vertebral column radiographs performed by the referring veterinarian revealed an expansile osteolytic lesion of the L2–L3 articular facet joint (Figure 1a). The cat was treated with meloxicam (0.05 mg/kg q24h PO [Loxicom; Norbrook]) and frunevetmab (1 mg/kg SC q28 days [Solensia; Zoetis]) for suspected spinal arthritis, and the cat's activity level increased initially.

General examination at our referral centre was unremarkable. On neurological examination, the patient had normal mentation and cranial nerve examination. The cat was non-ambulatory paraparetic with delayed postural reactions, normal withdrawal and hyperactive

[1]Fitzpatrick Referrals Orthopaedics and Neurology, Eashing, UK
[2]SYNLAB's Veterinary Pathology Group (VPG), Exeter, UK
[3]School of Veterinary Medicine, Faculty of Health and Medical Sciences, University of Surrey, Guildford, Surrey, UK
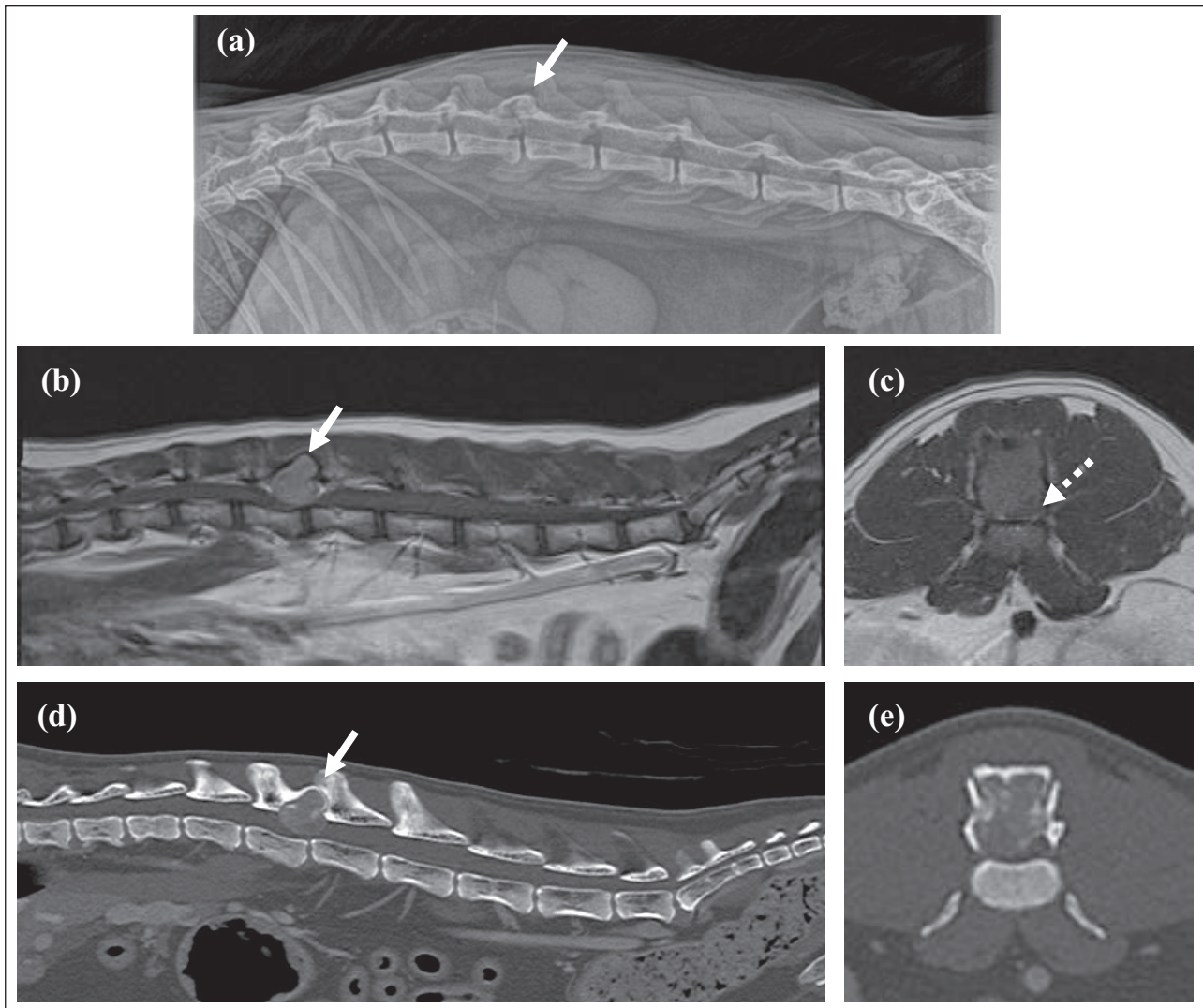[4]Wear Referrals, Bradbury, UK

Corresponding author:
Jordina Caldero Carrete MRCVS, Small Animal Teaching Hospital, Institute of Veterinary Science, University of Liverpool, Leahurst Campus, Chester High Road, Neston CH64 7TE, UK
Email: jordina.caldero@hotmail.com

Figure 1 (a) Radiograph, (b,c) MRI and (d,e) CT of the lumbar spine of a cat. (a) Right lateral radiograph of the lumbar vertebral column obtained 5 months prior to referral. There is an expansile, geometrically osteolytic lesion with preserved cortex at the L2–L3 articular facet joint resulting in a 'soap bubble' appearance (arrow). (b) Mid-sagittal T1-weighted imaging after gadolinium administration (T1WI + Gd) and (c) transverse T1WI + Gd at the level of the L2 vertebra. There is a large, well-defined extradural mass lesion with mild homogeneous contrast enhancement associated with the L2 lamina, caudal articular processes and right pedicle (solid arrow). The mass invades the vertebral canal, leading to severe right dorsolateral spinal cord compression (dotted arrow). (d,e) Mid-sagittal and transverse bone window CT after ioversol contrast at the level of the L2 vertebra showing the corresponding L2 mass of soft-tissue attenuation with moderate heterogeneous contrast uptake (arrow)

patellar reflexes on both pelvic limbs. Lumbar hyperaesthesia was detected. Neurological findings were consistent with a T3–L3 myelopathy. Based on the radiographic findings, a vertebral neoplasm (primary or metastatic) was considered the most likely differential.

Haematological parameters were unremarkable. Serum biochemistry revealed only slight hyperglycaemia (9.66 mmol/l; reference interval [RI] 3.95–8.84). Advanced imaging was indicated. MRI of the thoracolumbar spine was performed under general anaesthesia using a 1.5 Tesla MRI unit (Siemens Symphony Tim system). There was a single, well-defined, expansile extradural mass lesion (1.2 height × 1.4 length × 1 cm width) affecting the caudal half of the L2 lamina, caudal articular processes and right pedicle, which was expanded abaxially. The mass extended into the vertebral canal leading to severe right dorsolateral spinal cord compression. There was a focal, ill-defined intramedullary T2-weighted hyperintensity at this level. The mass had a heterogeneous appearance and was hypointense/isointense in T2-weighted images and isointense on T1-weighted sequences, with mild homogeneous contrast enhancement after gadolinium injection (0.1 mmol/kg [Dotarem; Guerbet Laboratories]) (Figure 1b,c). Images of the remaining neuroaxis revealed no further abnormalities.
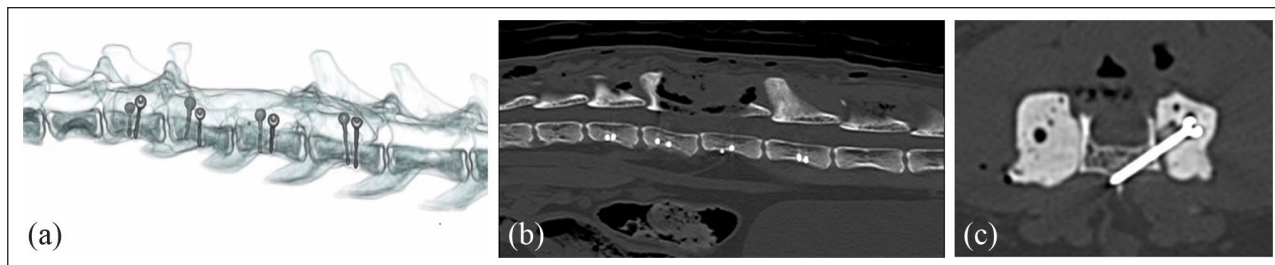
Figure 2 Postoperative mid-sagittal three-dimensional CT image of (a) the lumbar spine, (b) mid-sagittal bone window CT and (c) transverse bone window CT at the level of the L2 vertebra. En bloc excision of the tumour was performed, including part of the L2 and L3 spinous processes, L2–L3 articular facet joints and the majority of the pedicles. Titanium screws were placed bilaterally on the pedicles of L1, L2, L3 and L4, and embedded in polymethylmethacrylate cement

CT (160-slice Aquilion Prime; Toshiba) with ioversol contrast (2 ml/kg [Optiray 300; Guerbet Laboratories]) of the neck, thorax and abdomen was performed for the purpose of staging. In agreement with the MRI findings, CT identified an aggressive osteolytic lesion at L2 with strong ioversol contrast uptake (Figure 1d,e). Slight spondylosis deformans was present in between the L1 and L2 vertebrae. Other CT findings considered not clinically relevant included multifocal anaesthesia-related atelectasis, splenic parenchyma changes consistent with a benign process and bilateral elbow osteoarthrosis. There were no additional neoplastic foci.

Differential diagnosis of vertebral neoplasms included osteosarcoma (OSA), fibrosarcoma, chondrosarcoma, haemangiosarcoma, plasma cell tumours (multiple myeloma, plasmacytoma), histiocytic sarcoma and lymphoma. A benign bone tumour such as solitary or aneurysmal bone cysts could not be entirely excluded. The owner elected to pursue surgical management.

Preoperative surgical planning was performed by determining screw orientation and insertion within the bone corridors using a three-dimensional slicer software (Surgical Planning Lab, Harvard Medical School, Harvard University; www.slicer.org). A midline dorsal approach to the L1–L4 vertebrae was performed. The mass was removed by en bloc resection. A dorsal laminectomy was performed from the caudal portion of the L2 spinous process to caudal to the L3 spinous process, extending ventrolateral to the L2–L3 articular facet joints.[1] Vertebral stabilisation was performed using 1.5 mm titanium screws, which were placed bilaterally on the pedicles of L1, L2, L3 and L4 and embedded in polymethylmethacrylate (PMMA) cement. Implant entry points were estimated by visual approximation from the preoperative surgical planning video recording of the three-dimensional reconstruction, and drilling direction was guided by premeasured numeric values of inclination angles and osteotomy wedge gauges.

Haemostasis was controlled using Surgicel SNoW (Original Absorbable Hemostat; Ethicon). The exposed spinal cord was protected with local haemostatic agent (Lyostypt; Braun) and routine closure was performed.

Postoperative CT demonstrated correct placement of the implants and macroscopic resection of the tumour (Figure 2). The cat was discharged 5 days postoperatively, and, on discharge, was ambulatory paraparetic with moderate proprioceptive ataxia.

Histopathological examination of the mass demonstrated a densely cellular neoplasm expanding the vertebral bone. There was a thin cap of reactive woven bone around the periphery, and the neoplasm appeared contained within this. The neoplasm was formed of two cell populations: spindle cells and multinucleated giant cells (Figure 3a,b). Spindle cells predominated, and were arranged in a tightly interwoven storiform pattern surrounding small vessels and multifocally associated with islands and thin trabeculae of woven mineralised bone (Figure 3c). The spindle cells showed only mild pleomorphism without significant nuclear atypia. The multinucleated giant cells were sparse or densely scattered, and contained numerous (up to 50) nuclei that lacked significant atypia. Less than one mitosis was detected in 2.37 mm^2 (equivalent to 10 high-power fields) in both populations. Vascular invasion was not detected.

Immunohistochemistry with a histiocytic marker (ionised calcium binding adaptor molecule 1 [Iba1]; monoclonal AIF19mouse anti-Iba1 [Merck Millipore]), a general mesenchymal marker (vimentin [monoclonal mouse anti-vimentin, Clone V9; Dako]) and an osteoblast-specific transcription factor marker (osterix [polyclonal rabbit anti-Sp7/osterix; Abcam]) was performed.[2–7] The multinucleated giant cells exhibited weak cytoplasmic labelling with Iba1 (Figure 3d), suggestive of a monocyte/macrophage lineage. Most of the spindle cells showed nuclear labelling with osterix and both cell populations showed cytoplasmic labelling with vimentin (Figure 3e,f).

Based on the combined histological and immunohistochemical findings, the differential diagnosis included giant cell tumour of bone (GCTB) and giant cell-rich OSA. In consideration of the bland morphology of the cells, the absence of detectable mitotic activity and the apparent expansile rather than infiltrative growth pattern, a GCTB was favoured.
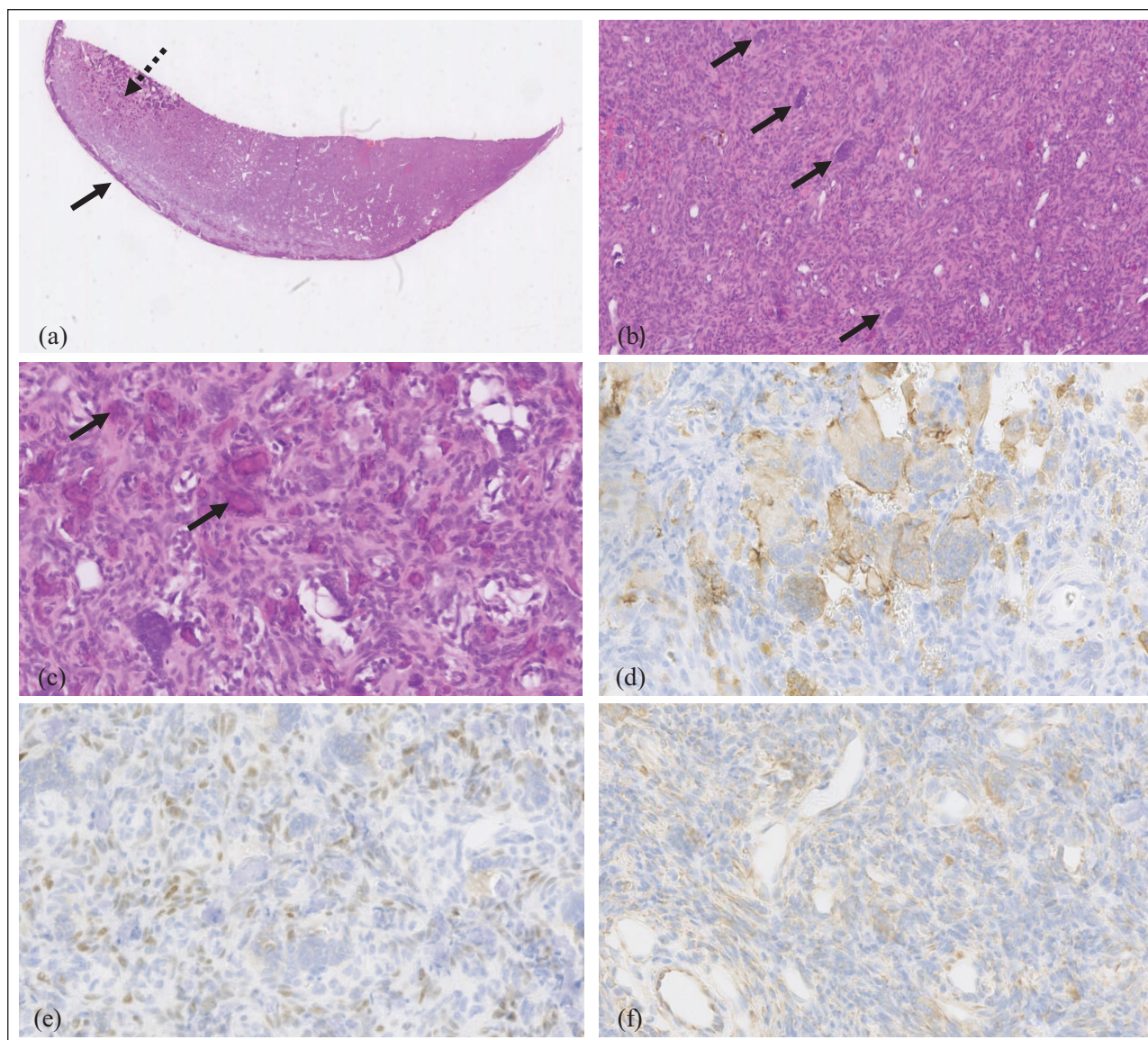
Figure 3 Histopathology of the bone lesion. (a) A thin cap of bone surrounds the tumour (arrow). There is bone production (dotted arrow; haematoxylin and eosin [H&E], × 10); (b) osteoclast-like multinucleated giant cells (arrows) appear distributed among a population of spindle-shaped mononuclear stromal cells (H&E, × 100); (c) the spindle cells surround small islands of woven mineralised bone (arrows). The spindle cells do not exhibit nuclear atypia or mitotic activity (H&E, × 400); (d) multinucleated giant cells show weak cytoplasmic labelling with ionised calcium-binding adaptor molecule 1, supportive of monocyte/macrophage lineage (3,3′-diaminobenzidine [DAB] chromogen [brown signal] with haematoxylin counterstain, × 400). (e) The majority of the spindle cells show nuclear labelling with osterix, supportive of osteoblast lineage (DAB chromogen [brown signal] with haematoxylin counterstain, × 400). (f) Both cell populations show cytoplasmic labelling with vimentin, a general mesenchymal marker (DAB chromogen [brown] with haematoxylin counterstain, × 400)

On re-examination 3 weeks postoperatively, the cat was ambulatory paraparetic with pelvic limb ataxia. Six months postoperatively, the cat returned to outdoor activity and had a good quality of life, although with a reduced ability to jump. The patient was ambulatory with subtle paraparesis. A postoperative full-body CT suggested instability of the L1–L4 spinal stabilisation construct demonstrated by multifocal PMMA fracturing and L2 implant loosening. Moderate periosteal reaction was present along the ventral/ventrolateral margins of L2–L3. There was no evidence of disease recurrence or metastasis.

Discussion

We report a GCTB in the vertebra of a cat. Unlike other primary bone tumours, GCTBs usually originate in the epiphyseal region of long bones.[8] In humans, GCTB is responsible for approximately 5% of all primary bone tumours and is typically located in the femur, tibia and radius.[9–13] Pelvic, sacral and spinal GCTBs are rare.[10,12,13]

Table 1 Stages of giant cell tumours of bone in humans, according to the Enneking staging system[37]

	Clinical features	Radiographic appearance	Histology
Stage I: latent	– Static, confined totally by bone; usually asymptomatic	– Well-defined margin and intact cortex – Surrounded by a capsule	– Histologically benign: benign cytology, clearly differentiated, low-to-moderate cell-to-matrix ratio
Stage II: active	– Progressing, expands bone or fascia – Symptomatic, often with pathological fracture	– Relatively well-defined margin, cortex thinned and moderately expanded – Evidence of bone and soft-tissue reactions	– Histologically benign
Stage III: aggressive	– Rapidly growing mass; invasive, breaches bone or fascia; may metastasise; symptomatic	– Indistinct borders and cortical destruction with soft tissue mass	– Histologically benign

According to the World Health Organization classification of soft tissue and bone tumours in 2020, GCTB was changed from a benign to an intermediate malignant tumour with locally aggressive behaviour and a high recurrence rate in humans.[14] Histologically benign pulmonary metastases occasionally occur in humans (1–9%).[13,15,16] Rarely, GCTB may undergo malignant transformation.[11,17]

GCTBs occur infrequently in animals.[18] GCTBs in cats have been reported in the mid diaphysis of the radius and tibia,[4,19] distal ulna and femur,[20–22] rib,[23] tibia[24] and digits.[25] Metastatic lesions occurred in the lungs, kidneys and subcutaneous flank.[4,21] All the cats were skeletally mature and duration of clinical signs varied from 2 to 20 weeks. Our findings agree with these features.

Canine GCTBs have been diagnosed as originating from the humerus,[26] accessory carpal bone,[27] scapula[28] and proximal tibia.[29] Metastases have been reported in regional lymph nodes, lungs, liver and other bones.[28,30] GCTBs have also been described in horses, laboratory rodents and avian species.[31–35]

Radiographically, GCTBs are characterised by expansile, osteolytic lesions with a geographical bone destruction pattern, usually surrounded by a thin bone shell. Sclerosis and periosteal new bone formation are typically not detected. Pathological fracture may occur.[18,36]

GCTBs have been classified in different stages based on clinical, histological and radiological features in human medicine. These are stage I (latent), stage II (active) and stage III (aggressive; Table 1).[37,38] Following this classification system, a stage II GCTB would have been attributed in this case.

Histologically, GCTBs have three main components: ovoid-to-spindle-shaped mononuclear stromal cells with a monotonous appearance; osteoclast-like multinucleated giant cells; and mononuclear cells of the monocyte/macrophage lineage.[11,14,39] The mononuclear stromal cells are believed to be derived from the osteoblast lineage and are the neoplastic component of the tumour.[18,40,41]

The giant cells in this tumour are labelled with Iba1. Other than Iba1 expression of tartrate-resistant acid phosphatase (TRAP)-positive osteoclast-like multinucleated giant cells in a feline uterine carcinosarcoma,[7] Iba1 labelling of osteoclasts is not widely reported. Unfortunately, TRAP was not available in this case. The histopathological analysis in our case is comparable to previous reports of feline GCTB.[4,19,20,22,23] The main differential was a giant cell-rich OSA, a histological subtype of osteosarcoma that also contains proliferations of giant cells.[18] The presence of a microscopic infiltrative pattern into adjacent bony trabecula, prominent lace-like osteoid deposition surrounded by osteoblasts, atypical pleomorphic spindloid cells with numerous mitotic figures and extra tumoral lymphovascular permeation would make a diagnosis of giant cell-rich OSA more likely.[18,42,43] The lack of periosteal reaction and absence of malignancy features supported the diagnosis of a GCTB.

The immunohistochemical findings helped to characterise the cells, although were not specific for GCTB. A GCTB-specific immunohistochemistry marker has been found in humans, but is not yet available in veterinary medicine.[39,44]

Differentiation between GCTB and OSA is important since most GCTBs have a favourable prognosis. Conversely, OSA is a malignant neoplasm that accounts for approximately 70% of all feline primary bone tumours. Although the clinical course of feline OSA is slower and metastases are less frequent than in its canine counterpart, prognosis varies depending on the location.[18,20,45,46] Median survival time for cats with axial OSA is lower (5.5–6.7 months) than for appendicular or extraskeletal OSA (49 months).[18,47] In our case, a rapid deterioration would have been expected with an OSA.

Surgery is the treatment of choice for spinal GCTBs in humans. Intralesional excision is indicated in stage II lesions, whereas piecemeal total spondylectomy or total en bloc spondylectomy is indicated in stage III lesions. Local recurrence is 6–17%.[13,48,49]

In small animals, only treatment for appendicular GCTBs has been reported and includes amputation or resection of the lesion. The 12-month follow-up revealed no recurrence or metastasis in three of these cases.[20,22,25,27] In a case report with a dog with a stage III tibial GCTB, local recurrence occurred 5 months after surgery.[29]

Following the human classification, this cat had a stage II GCTB and therefore our treatment approach should be considered appropriate.

Conclusions

The vertebra is an unusual site for GCTBs and it has not previously been reported in cats. This case report highlights GCTB as a relevant differential diagnosis in an elderly cat presenting with an expansile, lytic vertebral mass without metastasis. En bloc excision with vertebral stabilisation provided a satisfactory functional outcome and absence of local recurrence. Histopathological differentiation from a giant cell-rich OSA is challenging, but essential, since the prognosis varies significantly between these two neoplasms.

ORCID iD Clare Rusbridge (iD) https://orcid.org/0000-0002-3366-2110

References

1 Sharp NJH and Wheeler SJ. **Neoplasia.** In: Sharp NJH and Wheeler SJ (eds). Small animal spinal disorders: diagnosis and surgery. New York: Elsevier Mosby, 2005, pp 247–273.

2 Martín de las Mulas J, Espinosa de los Monteros A, Carrasco L, et al. **Immunohistochemical distribution of vimentin, desmin, glial fibrillary acidic protein and neurofilament proteins in feline tissues.** *Zentralbl Veterinarmed A* 1994; 41. DOI: 10.1111/j.1439-0442.1994.tb00059.x.

3 Pierezan F, Mansell J, Ambrus A, et al. **Immunohistochemical expression of ionized calcium binding adapter molecule 1 in cutaneous histiocytic proliferative, neoplastic and inflammatory disorders of dogs and cats.** *J Comp Pathol* 2014; 151: 347–351.

4 Ferreras MC, Fuertes M, Pérez V, et al. **Giant cell tumour of bone in a cat with extraskeletal metastases: pathological and immunohistochemical study.** *J Vet Med A Physiol Pathol Clin Med* 2005; 52: 225–229.

5 Nakashima K, Zhou X, Kunkel G, et al. **The novel zinc finger-containing transcription factor osterix is required for osteoblast differentiation and bone formation.** *Cell* 2002; 108: 17–29.

6 Flanagan-Steet H, Aarnio M, Kwan B, et al. **Cathepsin-mediated alterations in TGFß-related signaling underlie disrupted cartilage and bone maturation associated with impaired lysosomal targeting.** *J Bone Miner Res* 2016; 31: 535–548.

7 Murakami M, Yonemaru K, Goto M, et al. **Feline uterine carcinosarcoma infiltrated with osteoclast-like giant cells.** *J Vet Med Sci* 2022; 84: 1579–1584.

8 Jongeward SJ. **Primary bone tumors.** *Vet Clin North Am Small Anim Pract* 1985; 15: 609–641.

9 Turcotte RE. **Giant cell tumor of bone.** *Orthop Clin North Am* 2006; 37: 35–51.

10 Sobti A, Agrawal P, Agarwala S, et al. **Giant cell tumor of bone: an overview.** *Arch Bone Jt Surg* 2016; 4: 2–9.

11 López-Pousa A, Martín Broto J, Garrido T, et al. **Giant cell tumour of bone: new treatments in development.** *Clin Transl Oncol* 2015; 17: 419–430.

12 Bridge JA, Neff JR and Mouron BJ. **Giant cell tumor of bone. Chromosomal analysis of 48 specimens and review of the literature.** *Cancer Genet Cytogenet* 1992; 58: 2–13.

13 Tsukamoto S, Mavrogenis AF, Kido A, et al. **Current concepts in the treatment of giant cell tumors of bone.** *Cancers (Basel)* 2021; 13: 1–17. DOI: 10.3390/cancers13153647.

14 Flanagan AM, Larousserie F, O'Donnell PG, et al. **Giant cell tumour of bone.** In: WHO Classification of Tumours Editorial Board (eds). Soft tissue and bone tumours. Lyon: International Agency for Research on Cancer Press, 2020, pp 440–446.

15 Rock MG, Pritchard DJ and Unni KK. **Metastases from histologically benign giant-cell tumor of bone.** *J Bone Joint Surg Am* 1984; 66: 269–274.

16 Dominkus M, Ruggieri P, Bertoni F, et al. **Histologically verified lung metastases in benign giant cell tumours – 14 cases from a single institution.** *Int Orthop* 2006; 30: 499–504.

17 Beebe-Dimmer JL, Cetin K, Fryzek JP, et al. **The epidemiology of malignant giant cell tumors of bone: an analysis of data from the surveillance, epidemiology and end results program (1975–2004).** *Rare Tumors* 2009; 1: 159–163.

18 Thompson KG and Dittmer KE. **Tumors of bone.** In: Meuten DJ (ed). Tumours in domestic animals. Ames, IA: John Wiley & Sons, 2017, pp 356–424.

19 Walsh BA and Rhodes WH. **Giant cell tumor of bone in a cat.** *J Small Anim Pract* 1995; 36: 325–329.

20 Turrel JM and Pool RR. **Primary bone tumors in the cat: a retrospective study of 15 cats and a literature review.** *Vet Radiol Ultrasound* 1982; 23: 152–166.

21 Howard EB and Kenyon AJ. **Malignant osteoclastoma (giant cell tumor) in the cat with associated mast-cell response.** *Cornell Vet* 1967; 57: 398–409.

22 Bennett D and Duff RS. **Giant cell tumour of the ulna in a cat.** *J Small Anim Pract* 1983; 24: 341–345.

23 Thornburg LP. **Giant cell tumor of bone in a cat.** *Vet Pathol* 1979; 16: 255–257.

24 McClelland RB. **A giant-cell tumor of the tibia in a cat.** *Cornell Vet* 1941; 31: 86–87.

25 Wobeser BK, Kidney BA, Powers BE, et al. **Diagnoses and clinical outcomes associated with surgically amputated feline digits submitted to multiple veterinary diagnostic laboratories.** *Vet Pathol* 2007; 44: 362–365.

26 LeCouteur RA, Nimmo JS, Price SM, et al. **A case of giant cell tumor of bone (osteoclastoma) in a dog.** *J Am Anim Hosp Assoc* 1978; 14: 356–362.

27 Berg J, Gliatto JM and Wallace MK. **Giant cell tumor of the accessory carpal bone in a dog.** *J Am Vet Med Assoc* 1990; 197: 883–885.

28 Trigo FJ, Leathers CW and Brobst DF. **A comparison of canine giant cell tumor and giant cell reparative granuloma of bone.** *Vet Pathol* 1983; 20: 215–222.

29 Blondel M, Gros L, Semin M-O, et al. **A case of giant cell tumour of bone in a dog.** *VCOT Open* 2019; 2: 64–69. DOI: 10.1055/s-0039-3400513.

30 Garman RH, Powell FR and Tompsett JW. **Malignant giant cell tumor in a dog.** *J Am Vet Med Assoc* 1977; 171: 546–548.

31 May SA and Baker JR. **A giant cell tumour (osteoclastoma) of the tibia in a horse.** *Equine Vet J* 1985; 17: 477–479.

32 Imai T, Hibino N, Hayakawa K, et al. **Giant cell tumor of bone in an aged Fischer 344 rat.** *Toxicol Pathol* 1998; 26: 802–805.

33 Amann O, Meij BP, Westerhof I, et al. **Giant cell tumor of the bone in a scarlet macaw (*Ara macao*).** *Avian Dis* 2007; 51: 146–149.

34 Radaelli E, Rustighi A and Scanziani E. **Giant cell tumor of bonelike lesion in a Trp53 mutant mouse.** *Toxicol Pathol* 2012; 40: 675–681.

35 Gordon GE. **Osteoclastoma in a mare.** *Mod Vet Pract* 1974; 55: 540–541.

36 Mavrogenis AF, Igoumenou VG, Megaloikonomos PD, et al. **Giant cell tumor of bone revisited.** *SICOT J* 2017; 3: 54.

37 Enneking WF. **A system of staging musculoskeletal neoplasms.** *Clin Orthop Relat Res* 1986; 204: 9–24.

38 Campanacci M. **Giant-cell tumor and chondrosarcomas: grading, treatment and results (studies of 209 and 131 cases).** *Recent Results Cancer Res* 1976; 54: 257–261.

39 Noh BJ and Park YK. **Giant cell tumor of bone: updated molecular pathogenesis and tumor biology.** *Hum Pathol* 2018; 81: 1–8. DOI: 10.1016/j.humpath.2018.06.017.

40 Wülling M, Delling G and Kaiser E. **The origin of the neoplastic stromal cell in giant cell tumor of bone.** *Hum Pathol* 2003; 34: 983–993.

41 Cowan RW and Singh G. **Giant cell tumor of bone: a basic science perspective.** *Bone* 2013; 52: 238–246.

42 Chow LTC. **Fibular giant cell-rich osteosarcoma virtually indistinguishable radiographically and histopathologically from giant cell tumor-analysis of subtle differentiating features.** *APMIS* 2015; 123: 530–539.

43 Mallick A, Shah N, Mahmud S, et al. **Giant cell-rich osteosarcoma – a rare case.** *J Oral Maxillofac Pathol* 2020; 24 Suppl 1: 67–72.

44 Amary F, Berisha F, Ye H, et al. **H3F3A (Histone 3.3) G34W immunohistochemistry: a reliable marker defining benign and malignant giant cell tumor of bone.** *Am J Surg Pathol* 2017; 41: 1059–1068.

45 Ehrhart NP, Christensen NI and Fan TM. **Tumors of the skeletal system.** In: Vail DM, Thamm DH and Liptak JM (eds). Withrow & MacEwen's small animal clinical oncology. St Louis, MO: Elsevier, 2020, pp 524–564.

46 Dernell W, van Vechten B, Straw R, et al. **Outcome following treatment of vertebral tumors in 20 dogs (1986–1995).** *J Am Anim Hosp Assoc* 2000; 36: 245–251.

47 Heldmann E, Anderson M and Wagner-Mann C. **Feline osteosarcoma: 145 cases (1990–1995).** *J Am Anim Hosp Assoc* 2000; 36: 518–521.

48 Boriani S, Bandiera S, Casadei R, et al. **Giant cell tumor of the mobile spine: a review of 49 cases.** *Spine* 2012; 37: 37–45.

49 Tomita K, Kawahara N, Murakami H, et al. **Total en bloc spondylectomy for spinal tumors: improvement of the technique and its associated basic background.** *J Orthop Sci* 2006; 11: 3–12.